Modelling satellite galaxies in semi-analytical models

F.M. Delfino[1,2], C.G. Scóccola[1,2], C.A. Vega-Martínez[3,4] & S.A. Cora[1,2,5]

[1] *Facultad de Ciencias Astronómicas y Geofísicas, UNLP, Argentina*
[2] *Consejo Nacional de Investigaciones Científicas y Técnicas, Argentina*
[3] *Instituto de Investigación Multidisciplinar en Ciencia y Tecnología, Universidad de La Serena, Chile*
[4] *Departamento de Astronomía, Universidad de La Serena, Chile*
[5] *Instituto de Astrofísica de La Plata, CONICET–UNLP, Argentina*

Contact / fdelfino@fcaglp.unlp.edu.ar

Resumen / Entender la evolución de los halos satélites es importante para predecir la abundancia de subhalos de materia oscura y galaxias satélite. Sin embargo, en simulaciones numéricas de formación de estructura, pueden producirse disrupciones espurias que hacen que los halos de algunas galaxias no sean detectados. A estas galaxias que han perdido su halo de materia oscura se las denomina "galaxias huérfanas". En este trabajo, consideramos un modelo para la evolución de las órbitas de las galaxias huérfanas, que tiene en cuenta tanto los efectos de fricción dinámica como los de las fuerzas de marea. Se propone utilizar la función de correlación de dos puntos y la función de masa de halos de una simulación de N-cuerpos de alta resolución para acotar los parámetros libres del modelo.

Abstract / Understanding the evolution of satellite halos is important in predicting the abundance of dark matter subhalos and satellite galaxies. However, in numerical simulations of structure formation, spurious disruptions can occur that make the halos of some galaxies no longer detectable. Those galaxies that have lost their host dark matter halo are called "orphan galaxies". In this work, we consider a model for the evolution of the orbits of orphan galaxies, which takes into account the effects of both dynamical friction and tidal forces. We propose to use the two-point correlation function and the halo mass function of a high-resolution N-body simulation to constrain the free parameters of the model.

Keywords / galaxies: formation — galaxies: evolution — galaxies: halos — methods: numerical

1. Introduction

According to cold dark matter models of structure formation, galaxies form and evolve in dark matter (DM) halos. When accretions between DM halos that host galaxies occur, the most massive galaxy occupies the centre of the new halo and the least massive one becomes a satellite galaxy. While the satellite orbits its main system, it loses mass by tidal stripping and experiences dynamical friction, a drag force that gradually shrinks its orbit until it eventually merges with the central galaxy.

On the other hand, in numerical simulations of structure formation, it may happen that halo finders lose track of a satellite subhalo when it can no longer be distinguished as a self-bound overdensity within the larger system. This artifact is due to limited mass resolution and typically occurs at radius substantially greater than the separations from which the final galaxy merger is expected to occur. Satellite galaxies that lose their host subhalo, either by a merger with a larger structure or by artificial disruptions, and still persist in the simulation are called "orphan galaxies".

Since the evolution of satellite galaxies depends strongly on the orbit they describe within their host halo, a proper treatment of orphan satellites is important. In this work, we present an updated treatment for the orbits of orphan galaxies to be used in the SAG (Semi-Analytic Galaxies, Cora et al. 2018) semi-analytical model of galaxy formation and evolution.

2. Orbital evolution of orphan galaxies

2.1. Dynamical friction (DF)

When a satellite subhalo of mass M moves through a system composed of particles of mass $m << M$, it perturbs the particle field creating an over-dense region behind it. This "wake" pulls the subhalo in the opposite direction causing a net drag force called dynamical friction. The dynamical friction force is given by the Chandrasekhar formula (Binney & Tremaine, 2008), i.e.

$$\mathbf{F}_{\rm df} = -\frac{4\pi G^2 M^2 \rho(r) \ln\Lambda}{V^2}\left[\mathrm{erf}(X) - \frac{2X}{\sqrt{X}} e^{-X^2}\right]\frac{\mathbf{V}}{V}, \quad (1)$$

where r is the position of the satellite relative to its host halo, $\mathbf{V}$ is the velocity of the subhalo, $X = V/(\sqrt{2}\sigma)$ with σ the velocity dispersion of the dark matter particles, erf is the error function, ρ is the density of the host halo and $\ln\Lambda$ is the Coulomb logarithm. Here $\Lambda = b_{\rm max}/b_{\rm min}$ where $b_{\rm max}$ and $b_{\rm min}$ are the maximum and the minimum impact parameters for gravitational encounters between the satellite and the background objects.

We choose the following expression for $\ln\Lambda$

$$\ln\Lambda = \begin{cases} \ln(r/bR_{\rm sat}) & r > bR_{\rm sat} \\ 0 & r \leq bR_{\rm sat} \end{cases}, \quad (2)$$

where r is the distance from the subhalo to the center of the host halo, $R_{\rm sat}$ is the virial radius of the satellite and b is a free parameter. The previous expression for $\ln\Lambda$, proposed by Hashimoto et al. (2003), avoids the strong circularization effect that is observed when comparing these models with the results obtained from N-body simulations.

2.2. Tidal stripping (TS)

A subhalo orbiting within its host system is subjected to tidal forces. When tidal forces are greater than the gravitational force of the satellite itself, material become unbound and the satellite loses mass. We estimate the tidal radius as the distance at which the self-gravity force and the tidal forces cancel out, this is given by

$$r_{\rm t} = \left(\frac{GM}{\omega^2 - d^2\Phi/dr^2}\right)^{1/3}, \quad (3)$$

where M is the mass of the satellite, ω is its angular velocity and Φ characterize the potential of the host system (Taylor & Babul, 2001).

This equation is only approximately valid, because there are some particles within $r_{\rm t}$ that will be unbound while others outside $r_{\rm t}$ may remain bound to the subhalo. Also, the rate at which the material located outside of $r_{\rm t}$ is removed is not clear. Following Zentner et al. (2005), we absorb all these complicated details in a free parameter α to be adjusted by external constraints. Then we have

$$\frac{dM}{dt} = -\alpha\frac{M(>r_{\rm t})}{T_{\rm orb}}, \quad (4)$$

where $T_{\rm orb} = 2\pi/\omega$, with ω the instantaneous angular velocity of the satellite.

2.3. Merger criterion

According to hierarchical structure formation models, mergers play a critical role in the formation and evolution of galaxies. In this paper, we consider a satellite halo to be merged when the satellite-host distance is smaller than a fraction f of the virial radius of the main system, i.e. if $r_{\rm sat} < f\,R_{\rm host}$, where f is treated as a free parameter of the model.

3. Methodology

We use halo catalogs obtained from the DM only cosmological simulations MDPL2 and SMDPL. Both simulations follow the evolution of 3840^3 particles and are characterised by Planck cosmological parameters (Planck Collaboration et al., 2016). The simulation MDPL2 has a box size of $1.0\,h^{-1}$ Gpc which implies a mass particle of $1.5\times10^9\,h^{-1}\,{\rm M}_\odot$, while SMDPL has a box size of $0.4\,h^{-1}$ Gpc and a better mass resolution of $9.6\times10^7\,h^{-1}\,{\rm M}_\odot$. The DM halos were obtained with ROCKSTAR halo finder (Behroozi et al., 2013a), and their merger trees were constructed using CONSISTENT-TREES (Behroozi et al., 2013b).

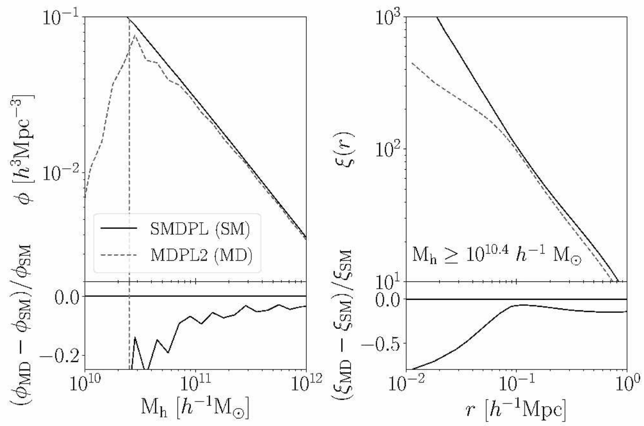

Figure 1: *Left panels:* HMF for the MDPL2 (red dashed line) and SMDPL (black solid line) simulations at redshift $z = 0$. *Right panels:* 2PCF (only for halos with masses greater than $10^{10.4}\ h^{-1}\,{\rm M}_\odot$) for the MDPL2 (red dashed line) and SMDPL (black solid line) simulations at redshift $z = 0$. Lower panels show the fractional difference between MDPL2 and SMDPL.

The left panels of Fig. 1 show the halo mass function (HMF, ϕ) for the SMDPL (solid line) and MDPL2 (dashed line) full simulations at $z = 0$. We note that for MDPL2, ϕ presents a break at ${\rm M_h} \sim 10^{10.4}\ h^{-1}\,{\rm M}_\odot$, which is the minimum mass from which we can guarantee that we have completeness in the number of halos for both simulations. Considering then halos with masses greater than $10^{10.4}\ h^{-1}\,{\rm M}_\odot$ in computing the corresponding two-point correlation functions (2PCF, ξ). These are shown in the right panels of Fig. 1 with solid and dashed lines for the MDPL2 and SMDPL simulations, respectively. The resulting clustering of SMDPL is greater than that of MDPL2 for all scales, being this effect more important for scales below 0.1 h^{-1} Mpc. This discrepancy is due to the greater fraction of satellite halos in SMDPL compared to MDPL2. To compensate for this lack of low-mass subhalos, once the subhalo of a galaxy is no longer detected by the halo finder algorithm we flag the satellite as orphan, and follow its orbital evolution applying the model presented in Sec. 2

To calibrate the free parameters of the model (b, f, α), we use information of ϕ and ξ taking the high resolution simulation SMDPL as a reference. We explore the parameter space to find the values that give an agreement between the results of the orbital model applied on MDPL2 and SMDPL. Since running the model over the full MDPL2 simulation is computationally very expensive, we select a small representative sub-volume of MDPL2 (MD50 hereafter). To this end, we divide MDPL2 in 8000 (20^3) disjoint sub-samples of boxsize 50 h^{-1} Mpc. From these sub-volumes, we select the box that better reproduces the HMF and 2PCF of the MDPL2 full simulation, optimizing for masses greater than $10^{10.4}\ h^{-1}\,{\rm M}_\odot$ and separations in the range $0.02 - 1\ h^{-1}$ Mpc. We then apply our model for the orbits of orphans into MD50 for different combinations of the parameters.

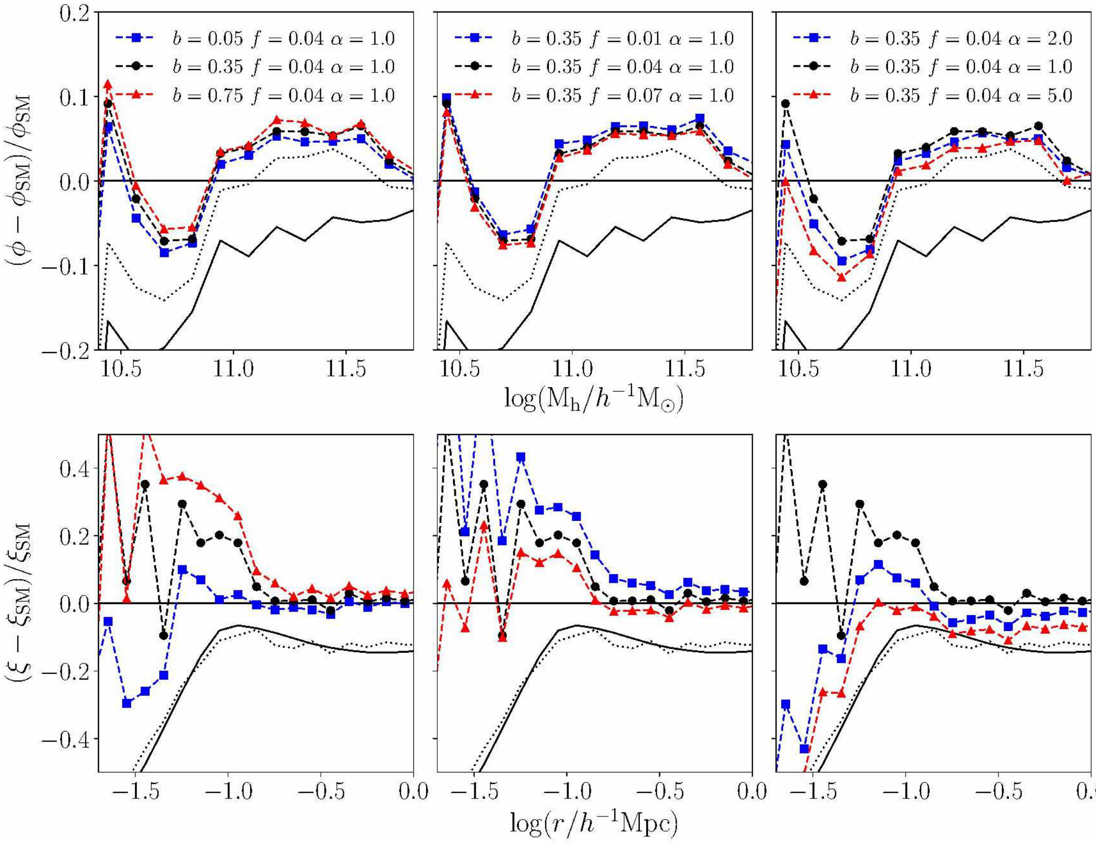

Figure 2: Fractional differences for HMF and 2PCF. The solid (black) line indicates the fractional difference for the MDPL2 simulation. The dotted (black) line indicates the fractional difference for the MD50 box. The dashed lines indicates the cases of MD50+model for different combinations of parameter. In all cases we took SMDPL as a reference to compute the fractional differences.

4. Results

Fig. 2 shows the results of running the orbital model on the MD50 sub-volume for different combinations of parameters (dashed lines plus symbols). In these figures we plot fractional differences taking SMDPL as a reference. Top panels show fractional differences for HMF while bottom panels show relative differences corresponding to 2PCF.

The left panels of Fig. 2 show (in dashed lines) the results of varying the parameter b leaving f and α fixed. Increasing the value of b is equivalent to decreasing the value of $\ln \Lambda$ (Eq. (1)), leading to a greater deceleration of the satellite halos due to dynamical friction (Eq. (2)). Therefore, if we reduce b, both ϕ and ξ decrease. On the other hand, a lower value of f implies fewer mergers and a greater number of satellite halos. Thus, both ϕ and ξ increase. This effect is shown in the middle panels of Fig. 2.

Finally, if we increase α then TS process is more efficient (Eq. (4)), we get a smaller fraction of satellite halos and ϕ decreases for all masses. Then, as we have a smaller fraction of satellites this also decreases ξ. This is shown in the right panels of Fig. 2. In general, we note that HMF is more sensitive to the variation of TS efficiency (α), while 2PCF seems to be sensitive to variations of the three parameters.

5. Conclusion

Clustering results show that low mass halos are responsible for the clustering difference between SMDPL and MDPL2 (Fig. 1). Therefore, we propose to use information of the 2PCF and HMF of a high resolution simulation (SMDPL) as constraints for the free parameters for the evolution model of orphan satellites. The results from the parameter exploration (Fig. 2) show that ξ is sensitive to variations of the three parameters (b, f, α) and can help to better define the parameters of the model. These preliminary results are soon to be published in full detail in Delfino et al. (2021).

References

Behroozi P.S., Wechsler R.H., Wu H.Y., 2013a, ApJ, 762, 109
Behroozi P.S., et al., 2013b, ApJ, 763, 18
Binney J., Tremaine S., 2008, *Galactic Dynamics: Second Edition*
Cora S.A., et al., 2018, MNRAS, 479, 2
Delfino F.M., et al., 2021, arXiv e-prints, arXiv:2102.01837
Hashimoto Y., Funato Y., Makino J., 2003, ApJ, 582, 196
Planck Collaboration, et al., 2016, A&A, 594, A13
Taylor J.E., Babul A., 2001, ApJ, 559, 716
Zentner A.R., et al., 2005, ApJ, 624, 505